Flow Turbulence Combust (2014) 93:125–140
DOI 10.1007/s10494-014-9540-x

Conditionally Statistical Description of Turbulent Scalar Mixing at Subgrid-Scales

Jian Zhang · Fujie Gao · Guodong Jin · Guowei He

Received: 11 November 2013 / Accepted: 17 April 2014 / Published online: 16 May 2014

Abstract Conditionally filtered passive scalar density function (FDF), dissipation (CFD), diffusion (CFDIF) and conditionally filtered velocity (CFV) are studied by using direct numerical simulation (DNS) data of homogeneous isotropic turbulent mixing with an imposed mean scalar gradient. The velocity and scalar fields are statistically stationary and have a Taylor micro-scale Reynolds number of 209. A three-dimensional box filter with a filter width of 21 scalar dissipation scales is employed to obtain filtered variables. The PDFs of conditioning variables, filtered scalar ($\langle\phi\rangle_L$), and subgrid-scale (SGS) scalar variance ($\langle\phi''^2\rangle_L$), are shown and are in reasonably good agreement with the experimental results of a one-dimensional filter. Since the three-dimensional filter has been used, the PDF of the filtered scalar exhibits perfect symmetry, and this significantly affects the symmetry of succeeding conditionally filtered statistics on $\langle\phi\rangle_L$ such as FDF, CFD, and CFDIF. The FDF, CFD, and CFDIF also show visible dependence on $\langle\phi''^2\rangle_L$. When $\langle\phi''^2\rangle_L$ varies from large to small, CFD varies from bell-shaped to U-shaped curves, and CFDIF varies from an inverse-S curve to a linear line; these are in accordance with the evolution of the FDF varying from bimodal to Gaussian. It suggests that the SGS mixing could be compared with global binary mixing in the view of the conditional description and this also suggests that it would reveal the non-equilibrium characteristics of the SGS scalar mixing; this SGS scalar mixing is supposed to be caused by diffusion-layer-like structures. In addition, the CFV remains linear regardless of the value of $\langle\phi''^2\rangle_L$. These results numerically confirm two distinct regimes of SGS mixing observed in previous experimental studies and extend the experimental results into isotropic turbulence, which suggests that the characteristics of the SGS scalar are intrinsic behavior of SGS mixing, independent of flow types.

Keywords Conditional statistics · Passive scalar mixing · Diffusion-layer-like structure · Direct numerical simulation · Turbulence

J. Zhang (✉) · F. Gao · G. Jin · G. He
LNM, Institute of Mechanics, Chinese Academy of Sciences, Beijing, 100190, China
e-mail: zhangjian@lnm.imech.ac.cn

1 Introduction

In recent decades, great efforts have been made to examine the large eddy simulation (LES) of turbulent combustion [8, 18]. In LES, the large, energy-containing scale velocity and scalar fields are directly solved from the filtered Navier-Stokes and scalar transport equations. The effects of the subgrid-scale (SGS) motions must be modeled. Meanwhile, the scalar diffusion and convection at unresolved scales are of great importance and must be well accounted for because they contribute significantly to the mixing of the fuel and oxidizer which of course controls the rate of reaction in most of the current combustion models, including the flamelet model [10, 19], the conditional moment closure (CMC) model [14, 24], the flamelet progress-variable (FPV) method [11, 12, 17], and the probability density function (PDF) method [3, 5].

The scalar PDF is usually used to statistically describe the turbulent mixing. In LES, however, the SGS turbulent mixing is represented by the scalar filtered density function (FDF), which is defined as

$$f_\phi(\hat{\phi};\mathbf{x},t)=\int \delta[\phi(\mathbf{x}',t)-\hat{\phi}]G(\mathbf{x}'-\mathbf{x})d\mathbf{x}'=\left\langle \delta[\phi(\mathbf{x},t)-\hat{\phi}]\right\rangle_L, \tag{1}$$

where $\hat{\phi}$ is the sample-space variable for the scalar ϕ, and δ is the Dirac delta function; G is a filter function. The integration is taken over the whole physical space. $\langle * \rangle_L$ denotes a resolvable-scale variable and L is the filter scale. The scalar FDF was called a subgrid-scale scalar PDF in earlier literatures [3, 4, 25]. It means the weighted distribution of the scalar in a subgrid cell and satisfies all the properties of a PDF for a given non-negative filter function [23]. The FDF of a passive scalar which measures the SGS turbulent mixing is needed in the LES of turbulent combustion to compute the filtered reaction rate as well as the filtered species mass fractions.

A widely used approach to obtain a scalar FDF is the assumed FDF method, which relates the SGS scalar distribution to its low order filtered moments. The beta function is mostly used to describe the SGS scalar distribution, and its parameters are determined by the filtered scalar and the SGS scalar variance [4, 25]. Additionally, the SGS scalar variance is computed from its transport equation.

The more systematic approach for determining the scalar FDF is to solve its transport equation, which is derived as [3, 26]

$$\frac{\partial f_\phi}{\partial t}+\frac{\partial}{\partial x_j}\{\left\langle u_j|\hat{\phi}\right\rangle_L f_\phi\}=\frac{\partial}{\partial x_j}\left(D\frac{\partial f_\phi}{\partial x_j}\right)-\frac{\partial^2}{\partial\hat{\phi}^2}\{\frac{1}{2}\left\langle \chi|\hat{\phi}\right\rangle_L f_\phi\}, \tag{2}$$

where D is the molecular diffusivity. In this equation, the conditionally filtered velocity (CFV), $\left\langle u_j|\hat{\phi}\right\rangle_L$, and the conditionally filtered scalar dissipation (CFD) , $\left\langle \chi|\hat{\phi}\right\rangle_L$, where $\chi = 2D\frac{\partial\phi}{\partial x_j}\frac{\partial\phi}{\partial x_j}$, are unclosed and still require modeling. Moreover, the conditionally filtered diffusion (CFDIF), $\left\langle D\nabla^2\phi|\hat{\phi}\right\rangle_L$, can be chosen as an alternative to CFD [26]. These unclosed terms continue to cause challenges.

In order to model these unclosed terms and determine a model of FDF, the statistical behaviors of SGS scalar mixing have to be figured out first. SGS turbulent mixing has received more attention through several experimental studies in recent years. [1, 2, 15, 23, 26–29]

Tong *et al.* [23, 26] experimentally studied the ensemble means of the scalar (temperature) FDF, CFD, CFDIF, and CFV conditioned on the resolvable-scale scalar and the SGS scalar variance with one-dimensional and two-dimensional data in a turbulent jet. (More

details will be given in Sec. 2.1). As the SGS scalar variance varies from large to small, the conditional means of the scalar FDF evolve from bimodal to approximately Gaussian, which is a locally binary mixing process that has not been observed in fully developed flows before. It suggests that, in the point of view of the conditional SGS scalar, the characteristics of scalar mixing are totally different from those shown by global statistics such as the scalar PDF which is unimodal and near Gaussian, and the scalar difference PDF which is stretched exponential.

The experimental results of Tong *et al.* provide a new insight toward systematically understanding SGS turbulent mixing, and toward modeling the unclosed terms in Eq. (2). Further study on this issue is therefore necessary. Three-dimensional data, which are difficult to measure experimentally, should especially be used to investigate these filtered statistical quantities. The main purpose of this paper is to use three dimensional data from a direct numerical simulation (DNS) to study the SGS scalar FDF, the conditional mean of the CFD, CFDIF, and CFV, as well as the SGS turbulent mixing.

DNS of a turbulent mixing flow resolves all of the turbulent and scalar scales and thus is frequently used to study scalar mixing. A number of works about turbulent mixing are based on the DNS of a passive scalar with an imposed scalar gradient, or with initially binary mixing fields in homogeneous and isotropic turbulence [6, 16, 21, 22, 30]. Using DNS data, Pumir [21] studied the PDF of a scalar gradient and revealed the occurrence of small regions where scalar gradients are very strong; Overholt and Pope [16] investigated the conditional mean of scalar dissipation. Scalar spectra and intermittency are also studied with DNS data [30]. Eswaran and Pope [6] investigated the influences of different length scales of the initial scalar fields on scalar mixing process by using the DNS data of homogeneous isotropic turbulent mixing flow, with an initial double delta distribution of the passive scalar. However, most of the studies numerically focus on the global statistical properties of a passive scalar (for instance, the scalar PDF, scalar dissipation rate, *etc.*). It is advantageous to use the DNS data to examine the SGS turbulent mixing.

The present paper is organized as follows. Section 2 summarizes the characteristics of experimental flows and implements a DNS of scalar mixing in which the characteristics of experimental flows are considered. In Section 3, we compare the conditional FDF, CFD, CFDIF, and CFV calculated from DNS data with experimental results and we discuss the properties of scalar mixing at subgrid-scales. Finally conclusions are summarized in Section 4.

2 Description of DNS

2.1 Flow conditions in experiments

The scalar FDF and unclosed terms in Eq. (2) were studied experimentally in a turbulent heated air jet with a fixed excess temperature between the jet exit and the room environment [23, 26]. The jet Reynolds number Re_j based on the nozzle diameter D_j and the jet exit velocity U_j was 40000, and the corresponding Taylor micro-scale Reynolds number Re_λ was approximately 220. Moving downstream, the scalar (temperature) mixing becomes fully developed. The measurement location of $x/D_j = 80$ was a significant distance into the fully developed region of the jet. Based on the jet Froude number, the buoyancy effect was negligible here; thus the temperature fluctuations were dynamically passive.

Since the jet nozzle produced a nearly top-hat velocity profile at the nozzle exit, the flow on the jet's centerline at the location of measurement could be approximated as a shearless

and homogeneous flow. Taylor's hypothesis was used to transform the signals of time series to spatial data for streamwise filtering. Primarily, one-dimensional filter data on the jet's centerline was used in the study.

Therefore, the fully developed, turbulent and homogeneous mixing of a passive scalar with a mean scalar gradient is the main characteristic of the experimental flow. It will be reflected in our direct numerical simulation and the one-dimensional hat filter in the experimental study is extended to a three-dimensional box filter in the present paper.

2.2 Computational details

Corresponding with the experiment flow characteristics, we consider the problem of scalar mixing by a turbulent flow spatially in three dimensions, with a mean scalar gradient. We define a constant mean gradient, β, in the Z direction, which coincides with a number of experimental situations; the scalar field is represented by the relation

$$\Phi(\mathbf{x}, t) = \phi(\mathbf{x}, t) + \beta Z, \tag{3}$$

where, ϕ is the fluctuating part of the scalar Φ, and the mean gradient β is -1. The passive scalar Φ in a turbulent flow is described by an advection-diffusion equation

$$\partial_t \Phi + (\mathbf{u} \cdot \nabla)\Phi = D\nabla^2 \Phi. \tag{4}$$

Substituting the relation of (3) into Eq. (4) yields the equation of the scalar fluctuation ϕ

$$\partial_t \phi + (\mathbf{u} \cdot \nabla)\phi = D\nabla^2 \phi - \beta u_z. \tag{5}$$

The last term of the right hand side in this equation βu_z effectively acts as a source of fluctuations, maintaining a steady state through a balance between the production (βu_z) and the diffusion ($D\nabla^2\phi$).

The DNS is implemented by numerically solving the Navier-Stokes equations

$$\partial_t \mathbf{u} + (\mathbf{u} \cdot \nabla)\mathbf{u} = -\nabla p + \nu \nabla^2 \mathbf{u}, \tag{6}$$

$$\nabla \cdot \mathbf{u} = 0, \tag{7}$$

along with Eq.(5).The pseudo-spectral method is applied for spatial differentiation, and the explicit second-order Adams-Bashforth method [30] is used for the time-stepping scheme. The periodic boundary conditions for the velocity and the scalar fluctuation, ϕ, are used in three directions. The periodicity length L_B is 2π in each direction, and these are equally divided by $N(= 512)$ grid points, so that the wavenumbers in the Fourier space are integers as $k_j = \pm n_j(2\pi/L_B) = \pm n_j$, where $n_j = 0, 1, ...N/2 - 1$ for $j = 1, 2, 3, \cdots$. The aliasing errors of the nonlinear terms are dealiased at each time step by the $\sqrt{2}/3$ rule.

The velocity field is initialized with a homogeneous and divergence free field, and assigned an initial energy spectrum

$$E(k) = Ck^{-5/3}, \tag{8}$$

where C is a constant assigned to 0.55 to obtain a specified initial kinetic energy. The initial scalar fluctuation field is set to a Gaussian distribution, and the initial scalar fluctuation spectrum is the same as the energy spectrum. During the iteration, the forces are added in both velocity and scalar fields at large scales in the wavenumber space ($|k| \leq 2$) to hold turbulent energy and scalar variance spectra consistent with $k^{-5/3}$ in the first two shells. This maintains a steady turbulent mixing state and produces a more extensive inertial range

for the velocity and scalar fluctuations to allow the investigation of the statistical properties of scalar fluctuations at a subgrid-scale. The artifacts introduced at low wavenumbers by the forces can be neglected in this study [16].

In order to monitor the resolution of a spectral simulation the product of the Kolmogorov length scale by the largest wave number, $k_{max}\eta$, is often used, and this should be greater than 1 in order to resolve the smallest scales of the flow velocity. For the cases of $Pr \leq 1$ in the DNS of passive scalar mixing, $k_{max}\eta \geq 1.4$ is typically used, since this seems sufficient to resolve the scalar field [21, 30]. To make a comparison with the experimental study, we considered the passive scalar as the air temperature, whose Pr number is around 0.7, and in the present simulation $k_{max}\eta$ equals 2.02, which means that the scalar is adequately resolved. The computational parameters of the DNS are presented in Table 1. The Taylor micro-scale Re number is 209 in the present simulation which is comparable with experimental condition of $Re_\lambda \sim 220$.

In this simulation, the velocity and scalar fluctuation fileds reach steady states after ~ 5 large eddy turnover times. The statistical samples of the velocity and scalar fluctuation fields are collected from $\sim$ 6 large eddy turnover times up to $\sim$ 9 large eddy turnover times, ensuring the convergence of the quantities to be investigated. The spectra of the scalar (temperature) and resolvable-scale scalar are plotted in Fig. 1. Here a box filter in a physical space is used with a filter scale of $\mathrm{L}/\eta_\phi = 21$ which is in the inertial scale range. This would make the results relevant to LES and allow the physics of the SGS mixing to be related to inertial range dynamics [2]. The lobes at higher wavenumbers are due to the leakage inherent to a box filter [23].

3 Results and Discussion

In this paper, in order to compare experimental results [23, 26], we will use a three-dimensional box filter in physical space. We will focus on the filtered scalar $\langle\phi\rangle_L$ and the SGS scalar variance $\langle\phi''^2\rangle_L$, where $\langle\phi\rangle_L$ is the local averaging over a grid of length L and $\phi'' = \phi - \langle\phi\rangle_L$ the SGS fluctuations. The filtered scalar and the SGS scalar variance can be used to determine the FDF as the cases for the assumed PDF method. We will first study the FDFs of $\langle\phi\rangle_L$ and $\langle\phi''^2\rangle_L$, and then their conditional filtering quantities, such as CFD,

Table 1 Summary of the computational parameters of DNS

Grid size, N^3	512^3
Taylor micro-scale Re number, Re_λ	209
Kolmogorov length scale, η	0.0084
Resolution, $k_{max}\eta$	2.02
Kinetic energy, E	1.15
Dissipation rate, ε	0.2
Large eddy turnover time, T_e	1.66
Prandtl number, Pr	0.7
Scalar variance, E_ϕ	1.51
Scalar dissipation rate, ε_ϕ	0.85

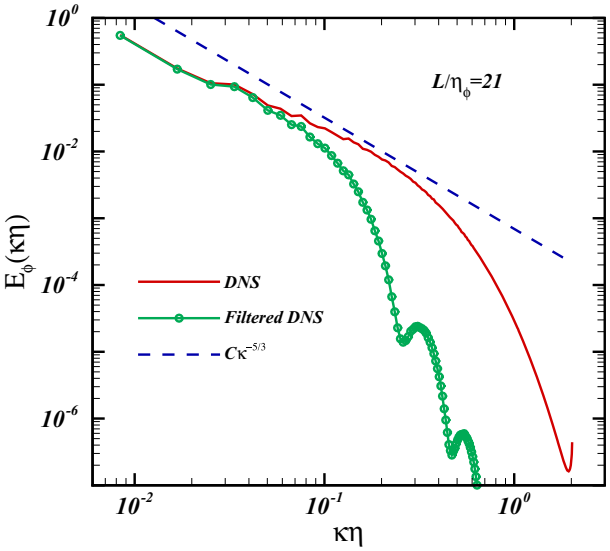

Fig. 1 The spectra of the scalar and resolvable-scale scalar from DNS of 512^3. The solid line is a scalar spectrum, and it has an inertial range corresponding to the $-5/3$ law (dashed line). The line with circles is the resolvable-scale scalar spectrum directly obtained from the filtered DNS with the filter width of $L/\eta_\phi = 21$ which is in the inertial scale range

CFDIF and CFV. To facilitate the comparison, all the quantities under this study are normalized using their $r.m.s$. For simplicity, $\langle\phi\rangle_L$, $\langle\phi''^2\rangle_L$, ϕ and ϕ'' are used to represent their corresponding normalized variables thereafter.

3.1 Basic statistics of the passive scalar

In the experiments [23, 26], Tong et al. proposed that the statistics of the FDF and the CFD,CFDIF, and CFV from a one-dimensional filter are expected to be as similar as two-dimensional and three-dimensional filters; thus the primary sources of differences between the experiment and the DNS are probably the conditioning variables $\langle\phi\rangle_L$ and $\langle\phi''^2\rangle_L$ whose statistics from one-dimensional and two-dimensional filters, and which can differ significantly. We first inspect the PDF of conditioning variables $\langle\phi\rangle_L$ and $\langle\phi''^2\rangle_L$ in order to examine the difference between one-dimensional and three-dimensional filters.

The PDF of ϕ and $\langle\phi\rangle_L$ are plotted in Fig. 2 (a). The PDF of $\langle\phi\rangle_L$ has almost the same shape as ϕ. The PDF of ϕ is close to Gaussian, which is consistent with Overholt and Pope's simulation [16]. Jaberi et al. [13] performed several DNSs of scalar mixing. Their results show that, for forced simulation in the presence of a mean scalar gradient, the scalar PDF will be close to Gaussian with a kurtosis slightly less than 3.0 which is near to present results of the kurtosis of 2.62 for scalar PDF.

Actually, the scalar PDF in Tong's experiment [23] of the scalar is super-Gaussian. Gylfason and Warhaft [9] measured the scalar PDF in grid turbulence and they show a super-Gaussian shape when wall effects are negligible and a sub-Gaussian shape when wall effects cannot be ignored. According to the experimental configuration, the wall effects can be neglected in Tong's experiment [23], and super-Gaussian PDF is reasonable. On the other hand, the forced simulation of turbulent mixing with a mean scalar gradient implies that it

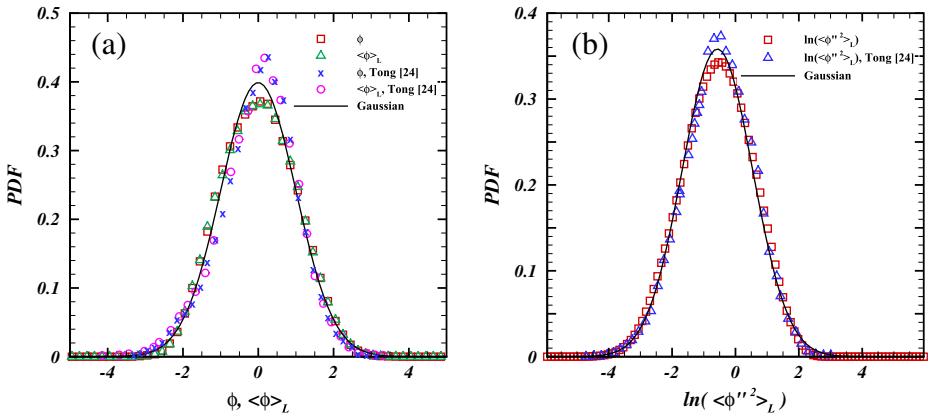

Fig. 2 **a** PDF of the passive scalar, ϕ, and the resolvable-scale passive scalar, $\langle\phi\rangle_L$, normalized by their *rms* respectively. **b** The PDF of the logarithm of the normalized SGS scalar variance. The thick lines represent Gaussian distributions with the same mean and variance as those of ϕ from DNS data

introduces the wall effect [7, 16]; therefore, there is a discrepancy between the experimental super-Gaussian scalar PDF and the numerical sub-Gaussian scalar PDF. In the present simulation the skewness of ϕ and $\langle\phi\rangle_L$ are 0.05; it is nearly zero rather than a negative value as it was in experiment [23, 26]. The PDFs of ϕ and $\langle\phi\rangle_L$ show perfect symmetry while experimental results negatively skewed, which could be expected to caused by different dimensions of the filters. For a complement, we calculate the skewness of ϕ and $\langle\phi\rangle_L$ from one-dimensional and two-dimensional filtered DNS data, and we find that the values are the same for one-dimensional and two-dimensional filters, that is, -0.18 for ϕ and -0.2 for $\langle\phi\rangle_L$, respectively. These results confirm that one-dimensional or two-dimensional filters lead to negatively skewed PDFs of ϕ and $\langle\phi\rangle_L$. Since $\langle\phi\rangle_L$ is a conditioning variable, it's symmetry would significantly affect the symmetry of succeeding conditional statistics.

According to the experiment [23], the PDF of $\langle\phi''^2\rangle_L$ is close to being log-Gaussian. Small differences still exist in that the PDF from DNS data is slightly sub-Gaussian, whereas slightly super-Gaussian in experiment [23]; this is probably attributable to different implicit conditions between numerical simulation and experiment as we interpreted above.

In the calculations of the conditional statistics, the five values of -2, -1, 0, 1, and 2, of the first conditioning variable $\langle\phi\rangle_L$ are used with the equal width bins. The SGS scalar variance at values of $\langle\phi''^2\rangle_L = 0.1$, 1.0, 3, 5, and 10 are chosen in this study. To ensure sufficient samples $\log_{10}\left(\langle\phi''^2\rangle_L\right)$ is divided into equal sub zones, and the widths of the bins are given by using proper number of zones for large and small SGS scalar variance values. The values and bins of the conditioning variables are chosen similarly to the way they were chosen for the experimental study [23, 26].

3.2 Conditional FDF

In this subsection, the means of the SGS scalar FDF conditioned on the filtered scalar $\langle\phi\rangle_L$ and SGS scalar variance $\langle\phi''^2\rangle_L$, $\left\langle f_\phi\left(\hat{\phi}\right) \mid \langle\phi\rangle_L, \langle\phi''^2\rangle_L\right\rangle$, are investigated and are given in Fig. 3, where the values of $\langle\phi\rangle_L$ are subtracted from the sample-space variable $\hat{\phi}$, and for convenience $\hat{\phi}$ is omitted in writing thereafter.

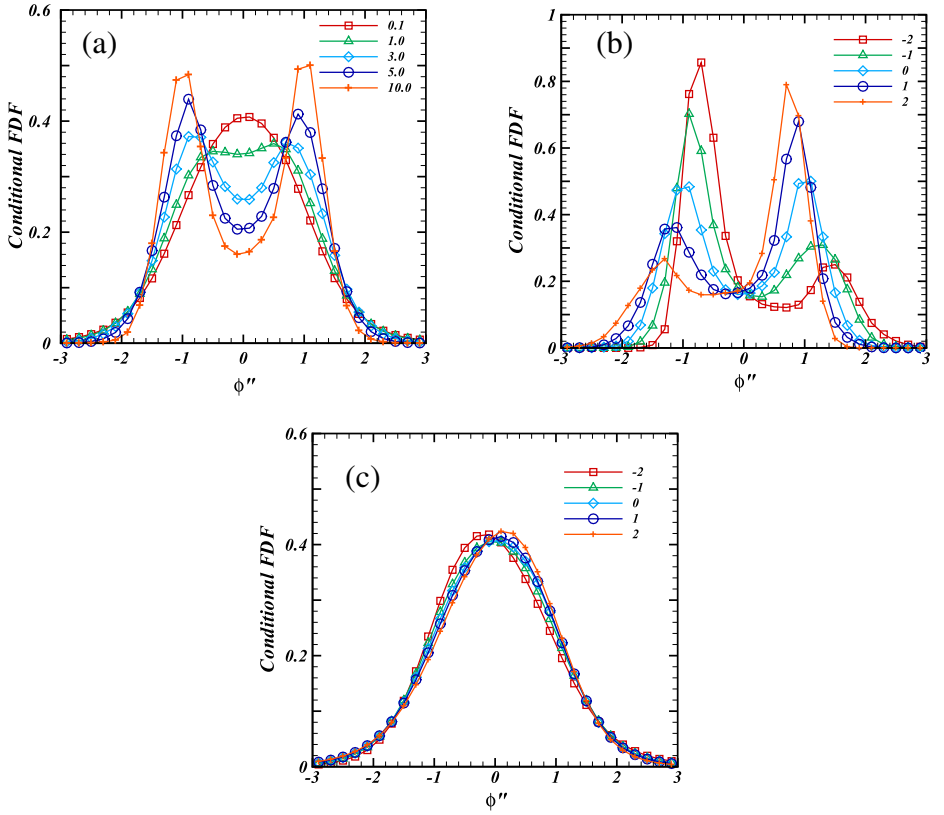

Fig. 3 Conditional mean of the scalar FDF. **a** The first conditioning variable $\langle\phi\rangle_L / \sqrt{\langle\langle\phi\rangle_L^2\rangle}$ equals 0, and the second one $\langle\phi''^2\rangle_L / \langle\phi''^2\rangle$ are given in the legend; **b** the filtered scalar are given in the legend, and the normalized SGS variance is 10; **c** the first normalized-conditioning variable is given in the legend, and the second normalized-conditioning variable is 0.1

As observed in Fig. 3 (a), for $\langle\phi\rangle_L = 0$, when $\langle\phi''^2\rangle_L$ is larger, the scalar FDF becomes distinct and symmetrically bimodal. As $\langle\phi''^2\rangle_L$ decreases, the scalar FDF evolves from bimodal to Gaussian, which is similar to the process of symmetrical, initial binary mixing [6], and which also is observed in experiment [23]. In addition, the present result shows excellent symmetry throughout, which can be expected, but has not been examined on an experimental basis. This improvement is primarily due to using a three-dimensional filter.

The SGS scalar shows bimodal distributions for all values of $\langle\phi\rangle_L$ at $\langle\phi''^2\rangle_L = 10.0$ in Fig. 3 (b) and shows the Gaussian distributions for all values of $\langle\phi\rangle_L$ at $\langle\phi''^2\rangle_L = 0.1$ in Fig. 3 (c). In Fig. 3(b), the FDF is systematically skewed. When $\langle\phi\rangle_L$ is taken as -2, the left peak of scalar FDF is obviously higher than the right peak. With the increase of $\langle\phi\rangle_L$, the left peak of the FDF becomes lower while the right peak becomes higher. When $\langle\phi\rangle_L$ goes to zero, the shape of the FDF tends to symmetry. Another kind of symmetry can also be seen in that the shape of scalar FDF at a positive value of $\langle\phi\rangle_L$ is symmetrical to that at an opposite value of $\langle\phi\rangle_L$. A similar symmetry also exists in Fig. 3(c) for approximately Gaussian distributions, but for a small SGS scalar variance the influence of the filtered scalar on the symmetry of the FDF shape is slight.

In the experiments [23, 26], the bimodal form of the conditional FDF corresponds to "locally binary mixing" and suggests a universal phenomenon in turbulent mixing. Here it is numerically verified by using a three-dimensional filter of a fully developed scalar field. According to Tong's analysis, the bimodal FDF is related to the diffusion-layer-like structure which is a region with a deep step change of scalar value; thus the diffusion-layer-like structure yields a sharp interface between relatively well-mixed regions. In order to examine the relationship between diffusion-layer-like structures and a bimodal scalar FDF, the means of the conditionally filtered dissipation rate that represent the local scalar gradient will be shown next.

3.3 Conditional CFD

In the method used in the conditionally statistical study, the conditional mean of the conditionally filtered dissipation rate is defined mathematically as $\left\langle \left\langle \chi \,|\phi''\right\rangle_L \,|\, \langle\phi\rangle_L \,, \left\langle\phi''^2\right\rangle_L \right\rangle$. It is normalized by $\left\langle \langle\chi\rangle_L \,|\, \langle\phi\rangle_L \,, \left\langle\phi''^2\right\rangle_L \right\rangle$ and plotted in Fig. 4. For small $\left\langle\phi''^2\right\rangle_L$ (typically less than 1), the conditional mean of the CFD is U-shaped in each figure of Fig. 4, and its value varies fairly small; they are close to one at the interval of $\left|\phi''\right| < 1$. The corresponding FDF shows a nearly Gaussian distribution, which indicates a relatively well-mixed and homogeneous SGS scalar field. As the SGS scalar variance becomes large, the conditional mean of the CFD is bell-shaped at values of $\left|\phi''\right|$ less than 1, and the bell peak changes to being higher and sharper for a larger $\left\langle\phi''^2\right\rangle_L$. Fig. 4 also shows that, for large SGS scalar variance, the conditional mean of the CFD is small when $\left|\phi''\right| > 1$ and less independent on ϕ''. The conditional mean of the FDF is bimodal-shaped for a large $\left\langle\phi''^2\right\rangle_L$, the valley of which between two peaks is of the same ϕ'' value as that of the bell peak of the corresponding CFD. The bimodal shape of the SGS scalar FDF is suggested to be related to the diffusion-layer-like structure that separates an SGS scalar field into two well-mixed parts. The main values of ϕ'' of the two parts correspond to the two peaks of the SGS scalar FDF. This means that the valley of the FDF corresponds to the diffusion-layer-like structure. The strong dissipation, which generally occurs in a diffusion-layer-like structure at the ϕ'' value of the valley of the FDF in Fig. 4, further confirms this inference.

On the other hand, the match between the conditional FDF and the conditional CFD is similar to that which occurs between the scalar PDF and the scalar dissipation in a developing turbulent mixing flow [6]. The scalar PDF in a developing scalar field which is initially binary mixing, is bimodal over short lengths of times; and the corresponding scalar variance is large; while the scalar dissipation rate shows a bell shape. Over time, the scalar PDF becomes approximately Gaussian with a decreasing value of scalar variance, while the scalar dissipation rate is U-shaped. The similarity between the locally binary mixing and the globally binary mixing, observed in experiments, is examined here using the DNS data.

The conditioning variable $\langle\phi\rangle_L$ affects the symmetry of the conditional mean of the CFD. For negative values of $\langle\phi\rangle_L$, CFD skews to positive ϕ'', and vice versa. For $\langle\phi\rangle_L = 0$, CFD is bilaterally symmetrical. The symmetry of the CFD that is dependent on $\langle\phi\rangle_L$ is evidently like that of the conditional FDF observed before.

The conditional CFD and FDF obtained using one-dimensional and two-dimensional filters are also plotted here in Fig. 5 to clarify the sensitivity of filter dimensions. Compared with Fig. 4, filter dimensions have a marginal impact on the conditional CFD and FDF, and this is in accords with the inference seen from experimental results [26]. Notably, the results from the three-dimensional filter present a better symmetry.

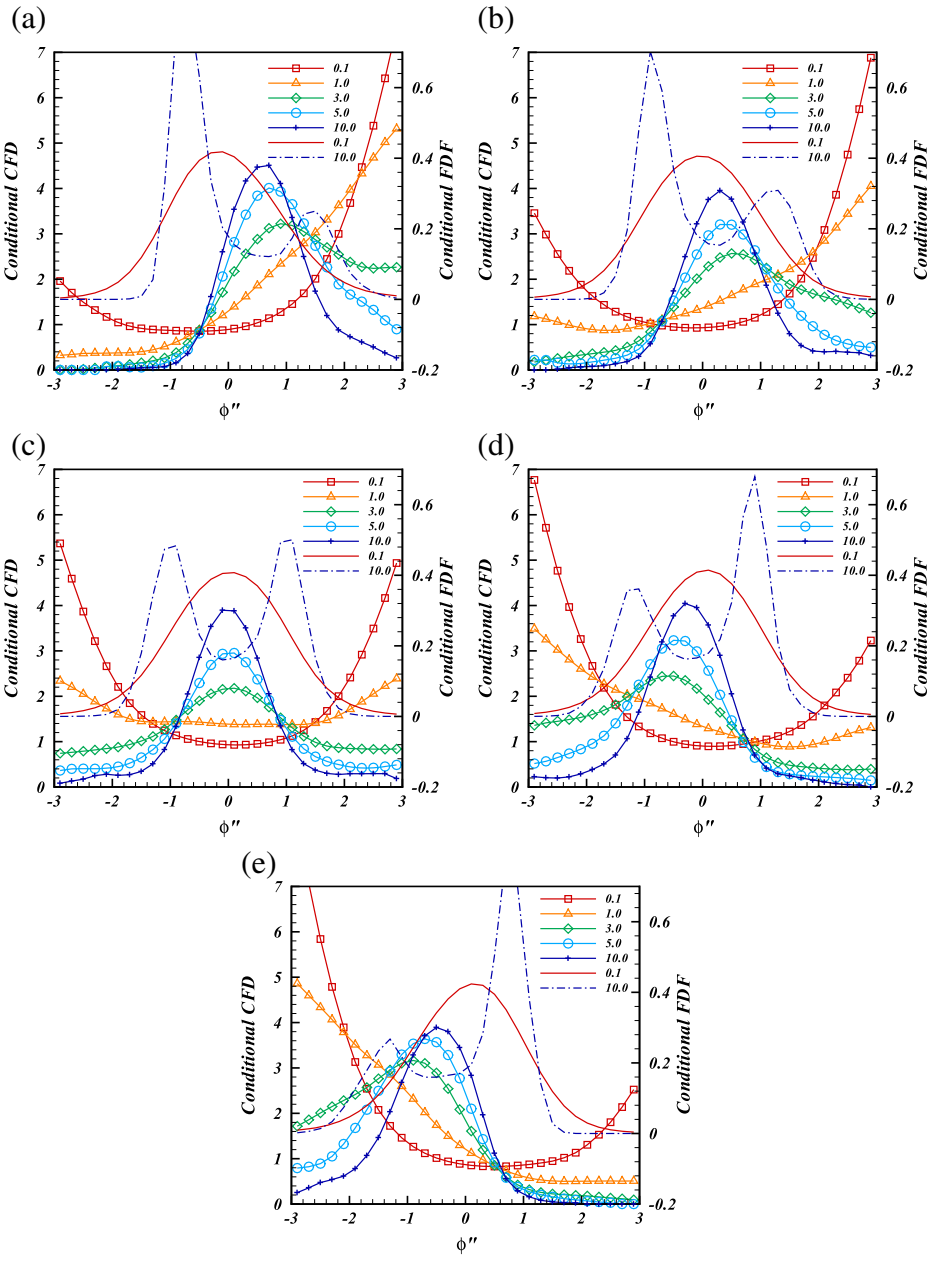

Fig. 4 Conditional mean of the CFD (lines with symbols). The values of the normalized $\langle\phi\rangle_L$ are (a)-2, (b)-1, (c)0, (d)1, and (e)2. The legend in each figure gives the values of $\langle\phi''^2\rangle_L$. The conditional mean of the SGS scalar FDF for the largest (dotted-dashed line) and the smallest (line with no symbols) values of $\langle\phi''^2\rangle_L$ are plotted for comparison

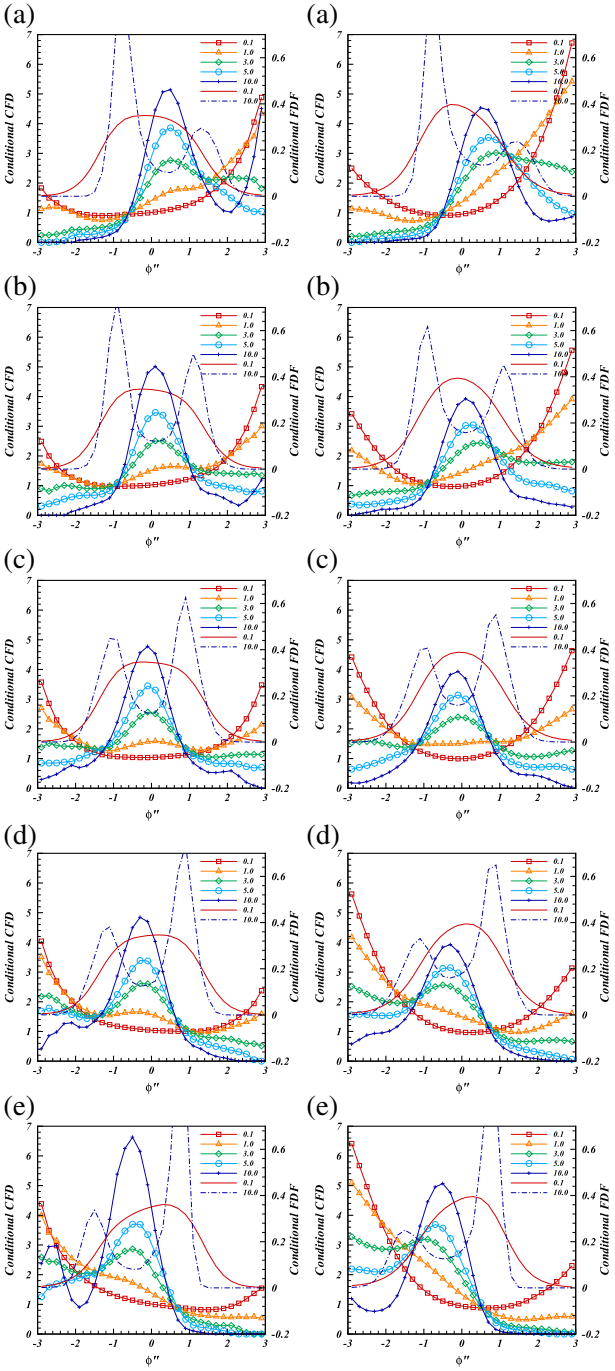

Fig. 5 Conditional mean of the CFD and FDF obtained using one-dimensional and two-dimensional filters. The values of the normalized $\langle\phi\rangle_L$ are (a)-2, (b)-1, (c)0, (d)1, and (e)2. The left column is from a one-dimensional filter, and the right column from a two-dimensional filter. Refer to the caption in Fig. 4 for the symbols and lines

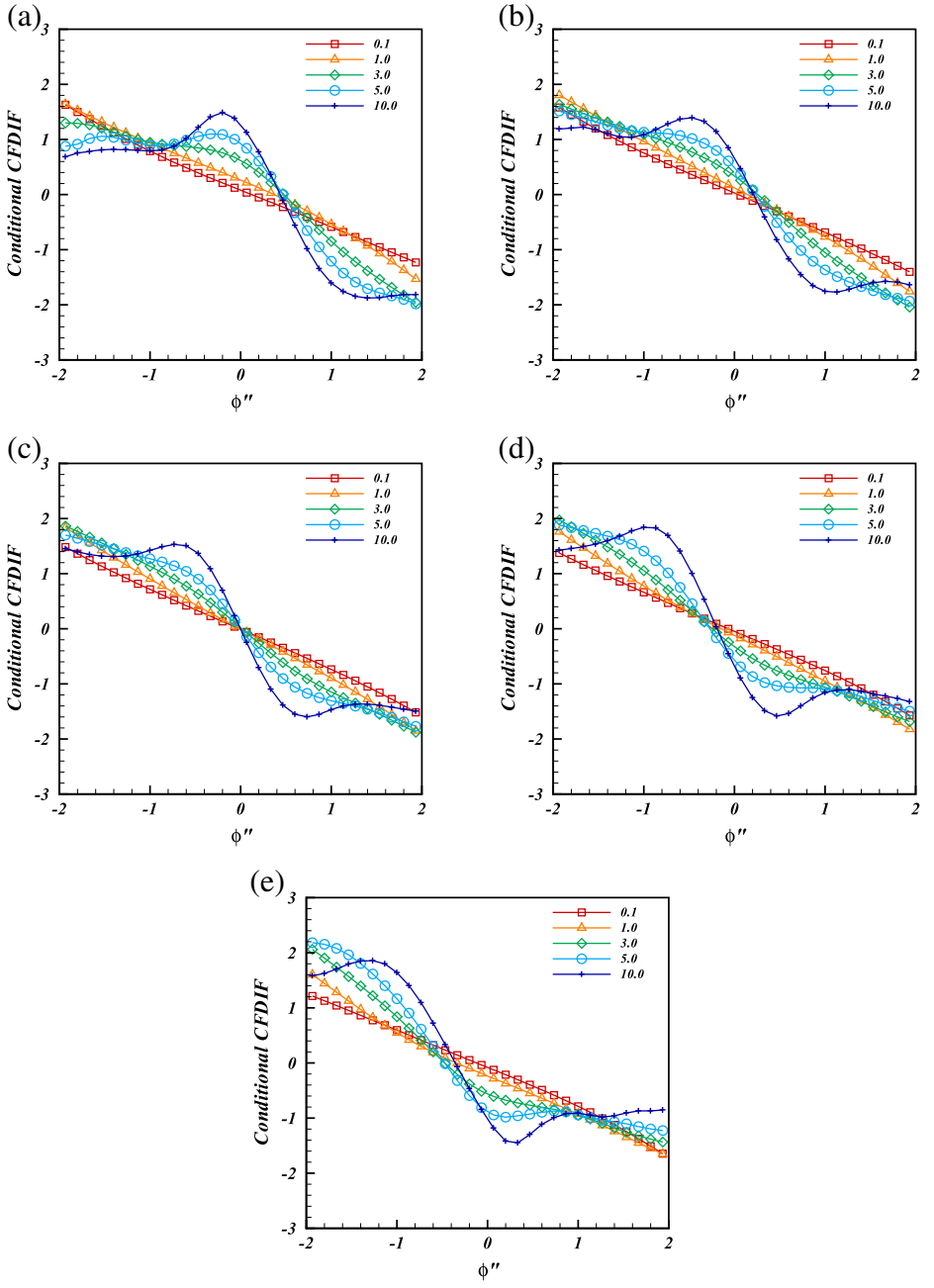

Fig. 6 Conditional mean of the CFD (lines with symbols). The values of the normalized $\langle\phi\rangle_L$ are (a)-2, (b)-1, (c)0, (d)1, and (e)2. The legend in each figure gives the values of $\langle\phi''^2\rangle_L$. The conditional mean of the SGS scalar FDF for the largest (dotted-dashed line) and the smallest (line with no symbols) values of $\langle\phi''^2\rangle_L$ are plotted for comparison

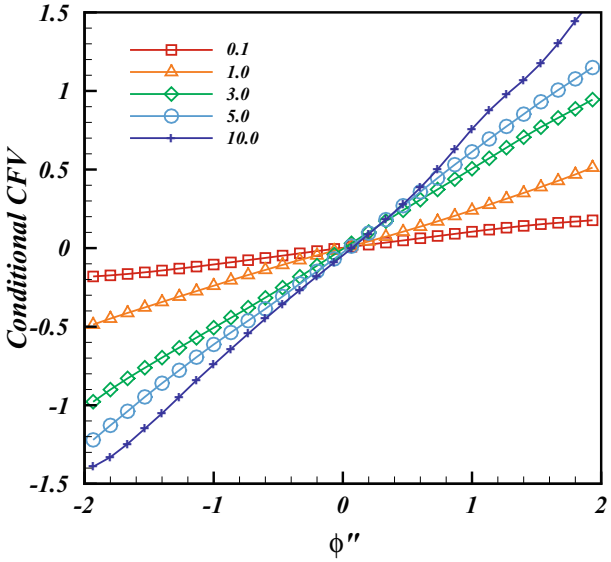

Fig. 7 The conditional means of the CFV with conditioning variable $\langle\phi\rangle_L = 0$. The SGS scalar variances are given in the legend

3.4 Conditional CFDIF

The conditional mean of the CFDIF, which is an alternative to the CFD in the SGS scalar FDF transport equation, Eq. (2), reads $\left\langle\left\langle D\nabla^2\phi|\phi''\right\rangle_L | \langle\phi\rangle_L, \left\langle\phi''^2\right\rangle_L\right\rangle$. It is normalized by $\left\langle\langle\chi\rangle_L / \sqrt{\left\langle\phi''^2\right\rangle_L} | \langle\phi\rangle_L, \left\langle\phi''^2\right\rangle_L\right\rangle$ and is shown in Fig. 6.

For a small SGS scalar variance value ($\left\langle\phi''^2\right\rangle_L = 0.1$), the conditional mean of the CFDIF is approximately linear, while the conditional mean of the FDF is approximately Gaussian (in Fig. 3c). This feature is similar to that shown in a DNS study of globally homogeneous mixing [16], where the PDF is approximately Gaussian and the conditional diffusion is linear. When $\left\langle\phi''^2\right\rangle_L$ increases, the scalar mixing deviates from a homogeneous status, and the conditional mean of the CFDIF no longer remains linear. When $\left\langle\phi''^2\right\rangle_L$ goes to the highest value, the conditional mean of the CFDIF shows a inverse-S curve. This phenomenon is in good agreement with the experimental results and is suggested to help interpret the effect of diffusion-layer-like structures on locally binary mixing [26] .

The conditioning variable $\langle\phi\rangle_L$ affects the curves of the CFDIF in the same way as the CFD. For $\langle\phi\rangle_L = 0$, all the curves are approximately centrally-symmetric on (0,0). For positive values of $\langle\phi\rangle_L$, the lines move towards the left side and vice versa. This symmetry is consistent with the FDF and the CFD, and is helpful to understand and model the locally binary mixing.

3.5 Conditional CFV

The filtered conditional SGS velocity $\left\langle\mathbf{u}''|\phi''\right\rangle_L$, instead of the filtered conditional velocity $\left\langle\mathbf{u}|\phi''\right\rangle_L$, where $\mathbf{u} = \langle\mathbf{u}\rangle_L + \mathbf{u}''$, is used here because the resolvable part of the velocity

is known in LES. The conditional mean of the CFV $\left\langle \left\langle w''|\phi'' \right\rangle_L | \langle\phi\rangle_L, \left\langle \phi''^2 \right\rangle_L \right\rangle$ along the direction of mean scalar gradient normalized by $\left\langle w''^2 \right\rangle^{1/2}$, is given in Fig. 7.

Figure 7 shows that the conditional CFV is approximately linear with ϕ'' for all $\left\langle \phi''^2 \right\rangle_L$ values. The slopes of the lines increase with the SGS scalar variance and all of them seem to cross the (0,0) point. For $\left\langle \phi''^2 \right\rangle_L = 0.1$, the line slope is close to 0. This means that the velocity fields have little influence on the SGS scalar field for well mixed subgrid volumes, while for large $\left\langle \phi''^2 \right\rangle_L$, the transport of the FDF by velocity fields becomes notable.

The linearity of the conditional mean of the velocity with the scalar fluctuations can be derived mathematically by using an assumed Gaussian scalar PDF [16, 20]. The linearity of the CFV with the SGS scalar also exists, which is possibly related to the approximately Gaussian FDF. It is remarkable that in a SGS scalar field with a bimodal FDF for a large $\left\langle \phi''^2 \right\rangle_L$, the CFV is still linear.

4 Conclusion

DNS with 512^3 grids of the homogeneous isotropic turbulent mixing flow, in the presence of an imposed mean scalar gradient, are implemented to study the FDF of a passive scalar, and the CFD, CFDIF, and CFV which are unclosed terms in the SGS scalar FDF transport equation. The Taylor micro-scale Reynolds number is 209. We take a three-dimensional box filter in the present study, and filter width typically is located in the inertial range of the scalar spectra. The following conclusions can be drawn from the present investigation:

• The scalar and filtered scalar PDFs are approximately Gaussian, and are similar to the results of experimental studies in jet flow [23]. The PDF of the logarithm of the normalized SGS scalar variance also exhibit similar to those of the experimental measurements. The three-dimensional filters provide a better symmetry for the PDF of filtered scalar in comparison with either one-dimensional or two-dimensional filters, which leads to better symmetry for the FDF, CFD, CFDIF, and CFV.

• The conditional means of the CFD and CFDIF are critically dependent on the second filtered moment of the SGS scalar $\left\langle \phi''^2 \right\rangle_L$. The CFD is bell-shaped for large $\left\langle \phi''^2 \right\rangle_L$ and becomes U-shaped for small $\left\langle \phi''^2 \right\rangle_L$. The conditional mean of CFDIF shows the consistent changes with decreasing $\left\langle \phi''^2 \right\rangle_L$, which varies from an inverse-S curve to a linear curve. These results are in accordance with the evolution of the mean of the FDF with $\left\langle \phi''^2 \right\rangle_L$. In addition, the dependence of the CFD on the SGS scalar variance is similar to that of the conditional dissipation on the scalar variance in globally binary mixing. The linear feature of the CFDIF is also similar to that of conditional diffusion in globally homogeneous mixing. The statistics conditioning on $\left\langle \phi''^2 \right\rangle_L$ in the SGS mixing processes are similar to the statistics in the global mixing processes.

• The numerical results of FDF and CFD confirm the two distinct regimes of SGS mixing that were previously observed experimentally in the literatures: the locally well-mixed SGS scalar with a Gaussian FDF, and the non-equilibrium SGS scalar with a bimodal FDF. The binary mixing at subgrid-scales is associated with diffusion-layer-like structures of scalar fields [26]. Diffusion-layer-like structure is also referred to as the ramp-cliff structure [21, 26]. It separates an SGS scalar field into two sub-domains with different means or variances, leading to a bimodal FDF at subgrid scales. The bell shape of CFD and the bimodal shape

of FDF suggest that the diffusion-layer-like structure represents the strongest dissipations, where large gradients play a role in connecting diffusion-layer-like structures with CFD and FDF.

• The conditional mean of the CFV linearly changes with $\langle \phi''^2 \rangle_L$ in the presence of a non-zero scalar gradient. For smaller $\langle \phi''^2 \rangle_L$, since the FDF is approximately Gaussian, the linearity of the CFV could be expected. This is analogous to the relation between the Gaussian PDF and linear conditional velocity. It is worth noting that, for larger $\langle \phi''^2 \rangle_L$, the FDF deviates from Gaussian and becomes a bimodal distribution. In this case, CFV still retains linearity.

• Finally, this work extends the previous experimental studies on SGS mixing in turbulence. On the one hand, the characteristics of the SGS scalar also exists in isotropic turbulence, suggesting that they are intrinsic behaviors of SGS mixing, independent of the flow type. On the other hand, the analyses employed a three-dimensional filter, whereas the previous experimental studies used one-dimensional and two-dimensional filters, demonstrating that the characteristics are independent of the filter dimension.

Acknowledgments This work was supported by 973 Program of China (2009CB724100, 2013CB834100) and NSFC (51376190, 50906096, 11072247, 11232011). This work was carried out at the National Supercomputer Center in Tianjin, and the calculations were performed on TianHe-1(A).

References

1. Cai, J., Barlow, R.S., Karpetis, A.N., Tong, C.: Conditionally filtered diffusion of mixture fraction and temperature in turbulent partially premixed flames. Proc. Combust. Inst. **33**, 1505–1513 (2011)
2. Cai, J., Wang, D., Tong, C., Barlow, R.S., Karpetis, A.N.: Investigation of subgrid-scale mixing of mixture fraction and temperature in turbulent partially premixed flames. Proc. Combust. Inst. **32**, 1517–1525 (2009)
3. Colucci, P.J., Jaberi, F.A., Givi, P., Pope, S.B.: Filtered density function for large eddy simulation of turbulent reacting flows. Phys. Fluids **10**(2), 381–396 (1998)
4. Cook, A.W., Riley, J.J.: A subgrid model for equilibrium chemistry in turbulent flows. Phys. Fluids **6**(8), 2868–2870 (1994)
5. Drozda, T.G., Wang, G., Sankaran, V., Mayo, J.R., Oefelein, J.C., Barlow, R.S.: Scalar filtered mass density functions in nonpremixed turbulent flames. Combustion and Flame **155**, 54–69 (2008)
6. Eswaran, V., Pope, S.B.: Direct numerical simulations of the turbulent mixing of a passive scalar. Phys. Fluids **31**(3), 506–520 (1988)
7. Ferchichi, M., Tavoularis, S.: Scalar probability density function and fine structure in uniformly sheared turbulence. J. Fluid Mech **461**, 155–182 (2002)
8. Fureby, C.: Towards the use of large eddy simulation in engineering. Prog. Aeronaut. Sci. **44**, 499–515 (2008)
9. Gylfason, A., Warhaft, Z.: On higher order passive scalar structure functions in grid turbulence. Phys. Fluids **16**(11), 4012–4019 (2004)
10. Hasse, C., Peters, N.: A two mixture fraction flamelet model applied to split injections in a di diesel engine. Proc. Combust. Inst. **30**, 2755–2762 (2005)
11. Ihme, M., See, Y.C.: Prediction of autoignition in a lifted methane/air flame using an usteady flamelet/progress variable model. Combust. Flame **157**, 1850–1862 (2010)
12. Ihme, M., Zhang, J., He, G., Dally, B.: Large-eddy-simulation of a jet-in-hot-coflow burner operating in the oxygen-diluted combustion regime. Flow, Turbul. Combust **89**, 449–464 (2012)
13. Jaberi, F.A., Miller, R.S., Madnia, C.K., Givi, P.: Non-guassian scalar statistics in homogeneous turbulence. J Fluid Mech **313**, 241–282 (1996)

14. Kronenburg, A.: Double conditioning of reactive scalar transport equations in turbulent nonpremixed flames. Physics of Fluids **16**(7), 2640–2648 (2004)
15. Liu, S., Tong, C.: Subgrid-scale mixing of mixture fraction, temperature, and species mass fractions in turbulent partially premixed flames. Proc. Combust. Inst. **34**, 1231–1239 (2013)
16. Overholt, M.R., Pope, S.B.: Direct numerical simulation of a passive scalar with imposed mean gradient in isotropic turbulence. Physics of Fluids **8**(11), 3128–3148 (1996)
17. Pierce, C.D., Moin, P.: Progress-variable approach for large-eddy simulation of non-premixed turbulent combustion. J Fluid Mech **504**, 73–97 (2004)
18. Pitsch, H.: Large-eddy simulation of turbulent combustion. Annu Rev. Fluid Mech **38**, 453–482 (2006)
19. Pitsch, H., Steiner, H.: Large-eddy-simulation of a turbulent pilotecd methane/air diffusion flame (sandia flame d). Phys. Fluids **12**(10), 2541–2554 (2000)
20. Pope, S.B., Ching, E.S.C.: Stationary probability density function: An exact result. Phys. Fluids, A **5**(7), 1529–1531 (1993)
21. Pumir, A.: A numerical study of the mixing of a passive scalar in three dimensions in the presence of a mean gradient. Phys. Fluids **6**(6), 2118–2132 (1994)
22. Samtaney, R., Pullin, D.I., Kosović, B.: Direct numerical simulation of decaying compressible turbulence and shocklet statistics. Phys. Fluids **13**(5), 1415–1430 (2001)
23. Tong, C.: Measurements of conserved scalar filtered density function in a turbulent jet. Phys. Fluids **13**(10), 2923–2937 (2001)
24. Ukai, S., Kronenburg, A., Stein, O.: Les-cmc of a dilute acetone spray flame. Proc. Combust. Inst. **34**, 1643–1650 (2013)
25. Wall, C., Boersma, B.J., Moin, P.: An evaluation of the assumed beta probability density function subgridscale model for large eddy simulation of nonpremixed, turbulent combustion with heat release. Phys. Fluids **12**(10), 2522–2529 (2000)
26. Wang, D., Tong, C.: Conditionally filtered scalar dissipation, scalar diffusion, and velocity in a turbulent jet. Phys. Fluids **14**(7), 2170–2185 (2002)
27. Wang, D., Tong, C.: Experimental study of velocity filtered joint density function for large eddy simulation. Phys. Fluids **16**(10), 3599–3613 (2004)
28. Wang, D., Tong, C.: Experimental study of velocity-scalar filtered joint density function for les of turbulent combustion. Proc. Combust. Inst. **30**, 567–574 (2005)
29. Wang, D., Tong, C., Barlow, R.S., Karpetis, A.N.: Experimental study of scalar filtered mass density function in turbulent partially premixed flames. Proc. Combust. Inst. **31**, 1533–1541 (2007)
30. Wang, L.P., Chen, S., Brasseur, J.G.: Examination of hypotheses in the kolmogorov refined turbulence theory through high-resolution simulations. part 2. passive scalar field. J. Fluid Mech **400**, 163–197 (1999)